RESEARCH ARTICLE

Theoretical analysis of frequency modulation-to-amplitude modulation on the final optics and target of the SG II-Up laser facility

Yujia Zhang [1,2], Wei Fan[1,2], Jiangfeng Wang[1,2], Xiaochao Wang[1,2], Xinghua Lu[1],

Dajie Huang[1], Shouying Xu[1], Yanli Zhang[1], Mingying Sun[1,2], Zhaoyang Jiao [1],

Shenlei Zhou[1,2], and Xiuqing Jiang[1]

[1] *Key Laboratory of High Power Laser and Physics, Shanghai Institute of Optics and Fine Mechanics, Chinese Academy of Sciences, Shanghai, China*

[2] *Center of Materials Science and Optoelectronics Engineering, University of Chinese Academy of Sciences, Beijing, China*

Abstract

Frequency modulation (FM)-to-amplitude modulation (AM) conversion is an important factor that affects the time–power curve of inertial confinement fusion (ICF) high-power laser facilities. This conversion can impact uniform compression and increase the risk of damage to optics. However, the dispersive grating used in the smoothing by spectral dispersion technology will introduce a temporal delay and can spatially smooth the target. The combined effect of the dispersive grating and the focusing lens is equivalent to a Gaussian low-pass filter, which is equivalent to 8 GHz bandwidth and can reduce the intensity modulation on the target to below 5% with 0.3 nm @ 3 GHz + 20 GHz spectrum phase modulation. The results play an important role in the testing and evaluating of the FM-to-AM on the final optics and the target, which is beneficial for comprehensively evaluating the load capacity of the facility and isentropic compression experiment for ICF.

Keywords: dispersion grating; frequency modulation-to-amplitude modulation conversion; high-power laser facility; inertial confinement fusion; phase modulation

1. Introduction

In order to optimize the laser–target interaction in inertial confinement fusion (ICF)[1,2], it is necessary to have precise control over the time–power curve and uniformity of each laser beam on the target. One of the technical challenges in time–power curve control is suppressing frequency modulation (FM)-to-amplitude modulation (AM)[3–5]. In high-power laser drivers, spectrum broadening technology based on sinusoidal phase modulation is required in the front-end system to avoid stimulated Brillouin scattering (SBS) in large-aperture optics[6] and achieve a smoother target intensity distribution. Ideally, pure phase modulation does not affect the temporal properties. However, when a frequency modulated laser transmits with a nonuniform

transfer function, the FM would convert to AM. For high-power laser facilities, each part of the facility (including the front-end system, the pre-amplification system, the main amplification system and the final optics assembly (FOA)) will produce a certain amount of FM-to-AM conversion[7]. The main sources of FM-to-AM conversion come from the front-end system, and include group velocity dispersion (GVD)[8] and polarization mode dispersion (PMD)[9] of long-transmission fiber and fiber devices, an uneven gain spectrum of the fiber amplifier[10] and a weak etalon effect[11]. The FM-to-AM conversion in the pre-amplifier system mainly occurs due to the gain narrowing caused by the nonuniform gain spectrum of the regeneration and multi-pass amplifier, as well as the removal of the sideband phase caused by the spatial dispersion of the smoothing by spectral dispersion (SSD) grating[12]. The main amplifier system of the SG II-Up facility adopts the configuration of 'large-aperture switch + four-pass cavity amplifier + two-pass booster amplifier'. The FM-to-AM conversion

Correspondence to: Wei Fan, Key Laboratory of High Power Laser and Physics, Shanghai Institute of Optics and Fine Mechanics, Chinese Academy of Sciences, Shanghai 201800, China. Email: fanweil@siom.ac.cn

mainly occurs due to gain narrowing and the pinhole of the spatial filter[13]. The FM-to-AM conversion of the FOA mainly comes from the frequency conversion, focusing lens and beam sampling grating (BSG).

Since the time–power curve control affects the optimal interaction of the laser–target and the intensity peaks caused by AM can damage the optics and affect laser performance, it is crucial to suppress the FM-to-AM conversion. The National Ignition Facility (NIF) in the United States uses 3 and 17 GHz to generate phase-modulated pulses with a spectral width of 0.3 nm. The NIF expects to achieve passive control of amplitude FM throughout the entire system to improve the reliability of FM-to-AM control. Single-polarization fiber[14] is used in the front-end system to effectively suppress the FM-to-AM conversion caused by PMD. A pair of bulk gratings is used to compensate for the FM-to-AM conversion caused by GVD in long-distance transmission fiber. In addition, birefringent filtering technology is used to compensate for the influence of gain inhomogeneity in the pre-amplifier system[15]. The Laser Mégajoule (LMJ) in France utilizes a two-stage waveguide phase modulator, operating at frequencies of 2 and 14.25 GHz, respectively, to generate phase-modulated pulses with a total bandwidth of 203 GHz and a spectral width of 0.75 nm. Different from the NIF, the front-end system of the LMJ utilizes polarization-maintaining fiber (PMF)[16,17]. The FM-to-AM control methods include using a shorter length of PMF, optimizing the PMF connector and axis alternation and inserting a polarizer. In addition, the LMJ also utilizes a dispersion compensation module made of Bragg grating to mitigate GVD[5].

The single-polarization fiber front-end system and PMF front-end system have been compared by the Shanghai Institute of Optics and Fine Mechanics, Chinese Academy of Sciences (CAS)[9]. According to the experimental results, the FM-to-AM modulation depth of the single-polarization fiber front end is suppressed to less than 3%, whereas the FM-to-AM modulation depth of the PM fiber front end is over 20%. The stability of the FM-to-AM modulation depth is 2% (peak–peak) and 0.38% (SD) over 3 h, which proves that the polarizing fiber front end is quite stable compared with the PM fiber system. The FM-to-AM conversion caused by GVD is compensated by a volume grating pair[8]. The gain inhomogeneity of the pre-amplification system and the main amplifying system is compensated by birefringence filtering technology[18].

The harm of FM-to-AM conversion includes an increased risk of damage to optical components, a disruption of the power balance and an increase in plasma instability. Therefore, real-time monitoring is necessary for the FM-to-AM conversion of laser pulses. The NIF initially required separate monitoring points for each channel. In addition, due to the need for a 34 GHz high-speed oscilloscope to sample the high-frequency signal on-site, it took over 12 h to complete the testing of 48 channels for FM-to-AM conversion[19]. Later, the LLNL (Lawrence Livermore National Laboratory) proposed Laser Screening at High-throughput to Identify Energetic Laser Distortion (SHIELD) in 2014[19]. Laser SHIELD can utilize a single 34 GHz oscilloscope to detect the variation in pulse peak power at 48 locations within a time frame of less than 1 second. It can also filter out non-compliant pulses and, for the first time, gather comprehensive data on FM-to-AM conversion at 48 pulse checkpoints simultaneously. Remote measurement of FM-to-AM conversion was also achieved by the Shanghai Institute of Optics and Fine Mechanics, CAS using wavelength conversion technology[20].

In order to evaluate the load capacity on the FOA and the effect of the FM-to-AM conversion on the time–power curve of the target, this paper analyzes the FM-to-AM conversion on the entire chain of the SG II-Up facility (Figure 1). The evaluation of temporal AM on the final optics and the target provides a theoretical basis for the FM-to-AM conversion monitoring, the load capacity evaluation and physical experiments conducting during the operation of the SG-II Up facility.

2. Phase modulation overview

2.1. Low-frequency phase modulation for suppressing transverse SBS of large-aperture optics

The high-power laser device with a single-frequency seed laser source has a high conversion efficiency, a smooth time–power curve and a good beam quality. However, the output power is limited by the transverse SBS effect of large-aperture optics. Phase modulation of the seed laser source produces a certain number of sidebands on both sides of the center frequency to reduce the optical power spectral density. When the spectral interval is smaller than the Brillouin gain bandwidth, the Brillouin gain spectrum produced by different sidebands superimpose on each other, which weakens the backward Stokes light and improves the SBS threshold of the system. The SG II-Up facility utilizes sinusoidal phase modulation at 3 GHz to achieve this effect. Without considering the initial low-frequency time shape of the pulse, the optical field can be expressed as follows[12,21]:

$$a_0(t) = \exp[im\sin(2\pi f_m t)]. \tag{1}$$

This is a periodic signal corresponding to a spectrum consisting of uniformly separated Dirac peaks:

$$\tilde{a}_0(f) = \sum_{n=-\infty}^{+\infty} J_n(m)\delta\left(f - nf_m\right), \tag{2}$$

where J_n is the nth-order Bessel function and the spectrum is composed of an infinite number of sidebands nf_m, each
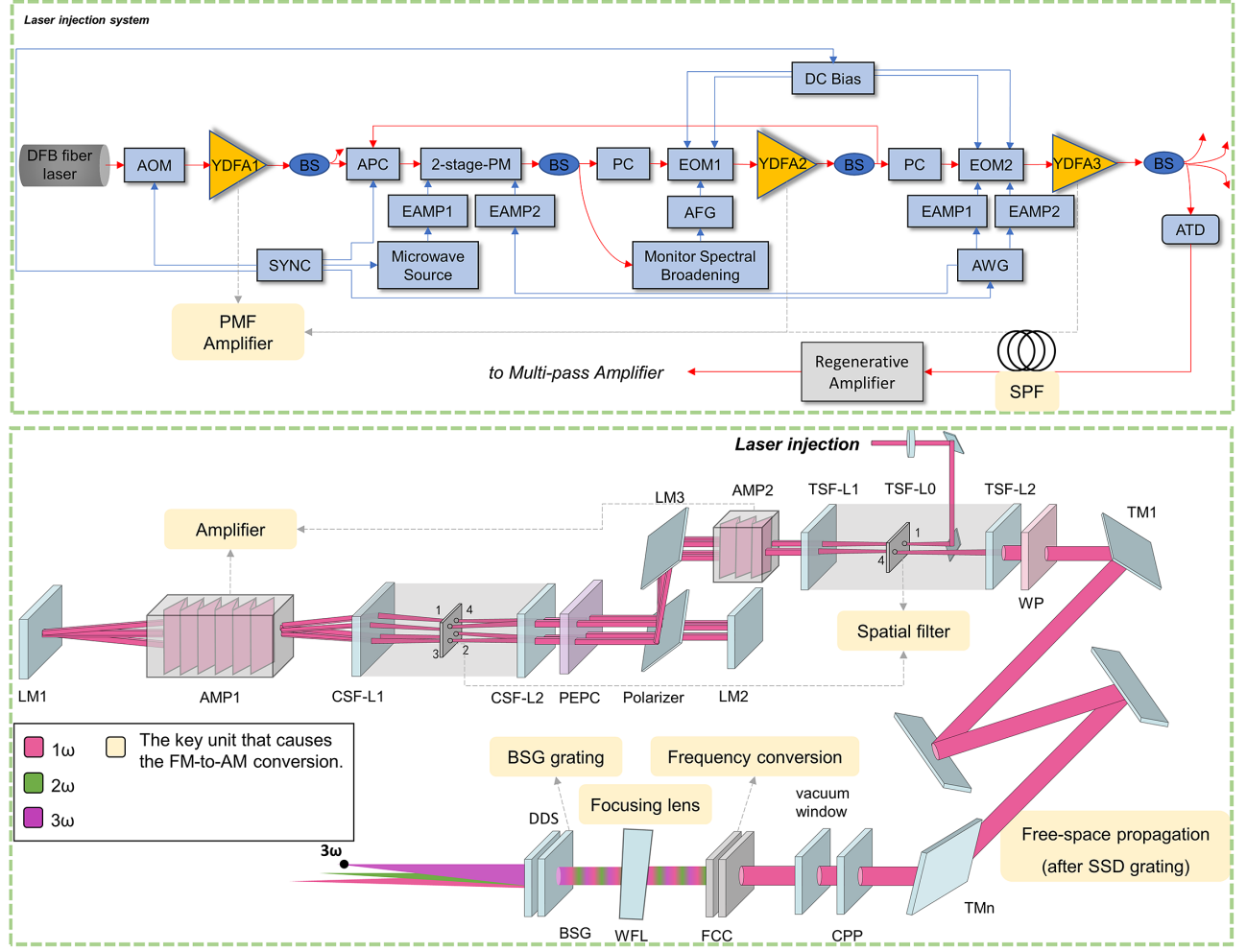
Figure 1. Schematic layout of the SG II-Up laser facility and the key unit that causes FM-to-AM conversion. DFB fiber laser, distributed feedback fiber laser; AOM, acoustic-optical modulator; YDFA, ytterbium-doped fiber amplifier; BS, beam splitter; APC, automatic polarization controller; 2-stage-PM, two-stage phase modulator; AFG, arbitrary function generator; AWG, arbitrary waveform generator; EOM, electro-optical modulator; SYNC, synchronization controller; EAMP, electric amplifier; ATD, adjustable time delay; CSF, cavity spatial filter; TSF, transmission spatial filter; AMP, amplifier; FCC, frequency conversion crystal; WFL, wedge focusing lens; BSG, beam sampling grating.

with a spectral density of $|J_n(m)|^2$, where 98% of the signal energy is contained within $2(m+1)f_m$.

2.2. High-frequency phase modulation for beam smoothing techniques

SSD technology is utilized to achieve the smoothing effect by employing spectral broadening pulses and dispersion systems to generate time-varying scattering spots. This approach helps maintain a homogenized intensity distribution after a certain integration time. The SG II-Up facility adopts target intensity control based on 'SSD+CPP' (CPP, continuous phase plate) technology. In order to achieve uniform beam design, starting from the requirements of the target focal spot, the specific parameters of the phase modulator and dispersion grating were determined. The technical approach for controlling the intensity distribution of a single-beam target is illustrated in Figure 2.

SSD can have a smoothing effect on the modulation of spatial scale less than $\Delta l = f\Delta\theta$ in the focal spot. From the target, we consider the target smooth size $\Delta l = 50\,\mu\text{m}$. The beam aperture at the SSD grating is $D_{\text{grating}} = 37$ mm, the target field triple frequency incident beam aperture is $D_{\text{T}} = 310$ mm, the focal length of the wedge focusing lens (WFL) is 2234 mm and the grating inscription is 1200 lines/mm. The unfolding angle between the edge frequency and the fundamental frequency at the WFL focal point is $\Delta\theta = \Delta l/(2f_{\text{WFL}}) = 11.19\,\mu\text{rad}$. It is known that the angular dispersion at the target field is $\zeta_{\text{DT}} = \zeta_{\text{grating}}\frac{cD_{\text{grating}}}{(\lambda/3)D_{\text{T}}} = 223.81\,\mu\text{rad/nm}$, and the angular dispersion rate at the grating is $\xi_{\text{grating}} = \frac{\Delta\theta(\lambda/3)D_{\text{T}}}{cD_{\text{grating}}(\Delta\lambda/3)} = 2.19 \times 10^{-9}$ s/m. The dispersion of the grating causes the laser pulse to introduce varying time delays at different spatial locations, and the total time delay is $t_{\text{d}} = \xi_{\text{grating}}D_{\text{grating}} = 81.2$ ps.

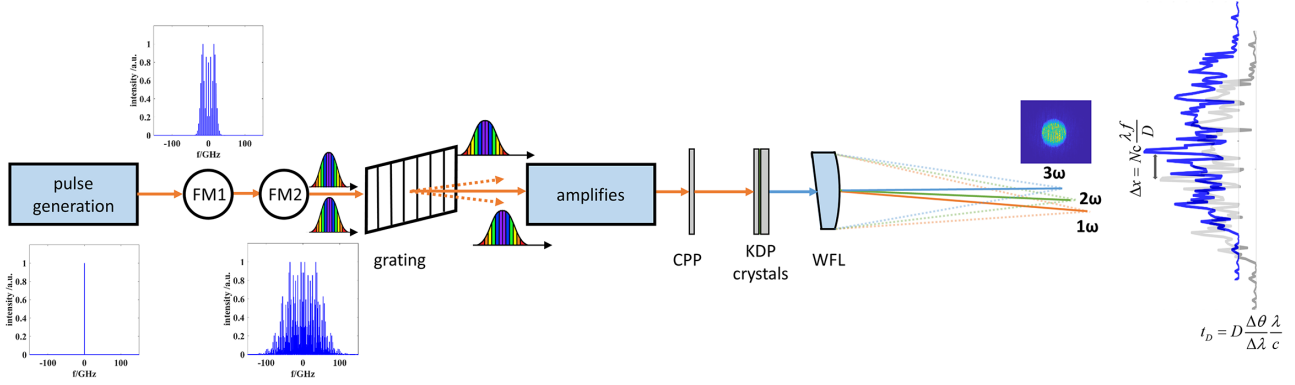The SG II-Up facility utilizes phase modulation at 3 GHz to suppress the transverse SBS of large-aperture optics and

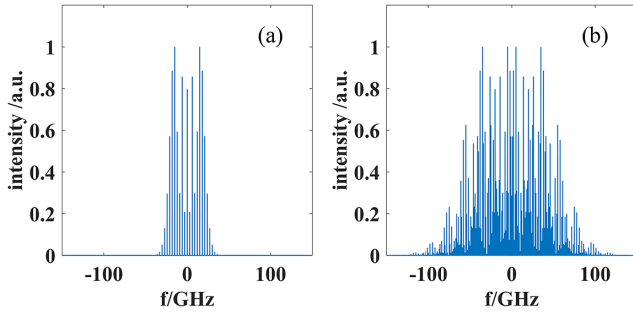**Figure 2.** Beam smoothing technology for a single laser beam.

Figure 3. (a) The 3 GHz sinusoidal phase modulation spectrum; (b) the 3 + 20 GHz sinusoidal phase modulation spectrum.

broaden the spectrum to 46.6 GHz@1053 nm. In addition, a 20 GHz phase modulation is employed to further broaden the spectrum to 121.2 GHz@1053 nm for beam smoothing. When the 3 GHz and 20 GHz phase modulators are combined, the resulting spectrum is their convolution, with a spectral width of 168 GHz@1053 nm. The spectral spreading caused by phase modulation is shown in Figure 3. Theoretically, pure phase modulation does not change the shape of the intensity, but it is inevitably affected by the nonuniform filtering of each of the optics during propagation, which produces intensity modulation. To quantify this concept, the modulation degree β is defined[5]. For single-frequency or multi-frequency phase modulation, no intensity modulation will be generated as long as the sideband phase remains constant:

$$\beta = \frac{I_{\max} - I_{\min}}{I_{\max} + I_{\min}}. \tag{3}$$

3. Frequency modulation-to-amplitude modulation conversion

3.1. Modulation degree calculation

In the case of single sinusoidal phase modulation, different AM spectral contents have varying effects on the damage of the optics and the laser–target interaction, even when the

value of β is the same. This is due to the filter function $H(f)$, which has an intensity spectrum as follows[5]:

$$\tilde{I}_{\text{out}}\left(kf_m\right) = \sum_{n=-\infty}^{+\infty} H^*\left(-nf_m\right)H\left[(k-n)f_m\right]J_{-n}(m)J_{k-n}(m). \tag{4}$$

Typically, the AM spectrum has the highest percentage of first-order harmonics, which have the greatest harmful effect on the laser–target interaction, considering all odd harmonics[5]:

$$\tilde{I}_{\text{out}}\left(kf_m\right) = \sum_{n=-\frac{k-1}{2}}^{+\infty} \left\{ H^*\left(nf_m\right)H\left[(k+n)f_m\right] \right. \\ \left. - H^*\left(-nf_m\right)H\left[-(k+n)f_m\right] \right\} J_n(m)J_{k+n}(m). \tag{5}$$

If $H^*\left(nf_m\right)H\left[(k+n)f_m\right] - H^*\left(-nf_m\right)H\left[-(k+n)f_m\right] = 0$, odd harmonics will not affect FM-to-AM conversion. To verify the equation, we can examine the properties between the Hermitian and anti-Hermitian functions:

$$H^*\left(-x\right) = \pm H(x). \tag{6}$$

So, for transfer functions that satisfy this condition, there are no odd harmonics of f_m in the AM spectrum, including the fundamental wave. During the transmission of a laser with a broadened spectrum, it is subject to an inhomogeneous phase or amplitude transmission.

3.1.1. Effect of the phase transfer function
Assuming that $H(f)$ is a purely imaginary number, it implies that only the phase of the laser pulse is affected by the transfer function. This relationship can be represented as follows[16]:

$$H(f) = \exp\left(-iaf^2\right). \tag{7}$$

Using the time-domain differentiation property of the Fourier transform, we can obtain the following:

$$a_{\text{out}}(t) = \int \tilde{a}_f \exp(i2\pi f t)\,df - \int \tilde{a}_f \left(iaf^2\right) \exp(i2\pi f t)\,df$$

$$= a_{\text{in}}(t) + \frac{ia}{4\pi^2} \frac{\partial^2 a_{\text{in}}(t)}{\partial t^2}. \tag{8}$$

Therefore:

$$a_{\text{out}}(t) = \exp\left[im\sin(2\pi f_m t)\right]$$
$$\times \left[1 - \frac{ia}{8\pi^2}(2\pi f_m)^2 m^2 - \frac{ia}{4\pi^2}(2\pi f_m)^2 m^2 \cos(4\pi f_m t)\right]$$
$$+ \frac{a}{4\pi^2}(2\pi f_m)^2 m \sin(2\pi f_m t). \tag{9}$$

Neglecting the higher-order terms, the incident light intensity can be derived as follows:

$$I_{\text{out}}(t) = 1 + \frac{a}{2\pi^2}\left[m\omega^2 \sin(\omega t)\right]. \tag{10}$$

Then the modulation degree is as follows:

$$\beta = \frac{am\,\omega^2}{2\pi^2}, \tag{11}$$

where m represents the phase modulation degree and $\omega = 2\pi f_m$, where f_m is the modulation frequency. The modulation degree caused by the change of the phase transfer function is proportional to the phase modulation degree and the square of the modulation frequency.

3.1.2. Effect of the amplitude transfer function

If the intensity response of the transmission medium to the pulse is expressed as follows[16]:

$$H_{\text{amplitude}}(f) = 1 - \sigma_f(f - f_c)^2, \tag{12}$$

where f_c represents the central frequency of the intensity response and σ_f represents the bandwidth of the intensity response; then, without considering the phase effect, the transfer function of the amplitude can be expressed as follows:

$$H_{\text{amplitude}}(f) = 1 - \frac{1}{2}\sigma_f(f - f_c)^2, \tag{13}$$

$$a_{\text{out}}(t) = \int \tilde{a}(f)\left[1 - \frac{1}{2}\sigma_f(f - f)^2\right]\exp(i2\pi f)\,df. \tag{14}$$

It can be transformed equivalently as follows:

$$a_{\text{out}}(t) = a_{\text{in}}(t) - \frac{1}{2}\sigma_f \exp(i2\pi f_c t)\int \tilde{a}\left(\widehat{f}\right)\left(\widehat{f} - f_c\right)^2$$
$$\times \exp\left[i2\pi\left(\widehat{f} - f_c\right)t\right]d\left(\widehat{f} - f_c\right). \tag{15}$$

Let $\widehat{f} - f_c = f$, and by utilizing the time-domain differential property of the Fourier transform and the displacement

property, while neglecting the higher-order terms, we ultimately derive the following:

$$I_{\text{out-modulation}}(t) = 1 - \sigma_f\left[f_c - mf_m \cos(2\pi f_m t)\right]^2. \tag{16}$$

The modulation signal is as follows:

$$I_{\text{out-modulation}}(t) = \sigma_f\left[f_c - mf_m \cos(2\pi f_m t)\right]^2. \tag{17}$$

When $f_c < mf_m$, the modulation degree is as follows:

$$\beta = \frac{\sigma_f\left(f_c + mf_m\right)^2}{2 - \sigma_f\left(f_c + mf_m\right)^2}. \tag{18}$$

When $f_c > mf_m$, the modulation degree is as follows:

$$\beta = \frac{2\sigma_f mf_m f_c}{1 - \sigma_f\left(f_c^2 + m^2 f_m^2\right)}. \tag{19}$$

Figure 4 shows the intensity spectrum of these two transfer functions. The first column represents the amplitude transfer function, the second column represents the phase transfer function and the third column represents the AM spectrum. It can be observed that the modulation degrees of the two transfer functions are nearly identical, although they are caused by different spectral components. Considering the phase modulation only at 20 GHz, for the pure phase transfer function $\exp\left(i\sigma f^2\right)$ (as shown in Figure 4(a)), the AM spectrum contains integer multiples of f_m, such as 20, 40 and 60 GHz. The modulation degree is primarily influenced by the fundamental- or low-frequency component.

For the pure amplitude transfer function, three cases are considered. The first case is the symmetric amplitude transfer function $\exp\left(\sigma f^2\right)$ (as shown in Figure 4(b)). The AM spectrum of this case satisfies the relation of Equation (5), and there are no odd harmonics of f_m. The second is the asymmetric exponential amplitude transfer function $\exp\left[\sigma(f - f_c)^2\right]$ (as shown in Figure 4(c)). The AM spectrum of this case has an additional effect of 20 GHz compared to the first case. It is known that the modulation generated by translation is mainly caused by the fundamental frequency f_m. The third category is the linear amplitude transfer function $\sigma f + f_c$ (as shown in Figure 4(d)). The AM spectrum of this function mainly consists of the odd harmonics of f_m. In addition, in the laser–target interaction, the lower frequency effect is often more detrimental, and thus the whole AM spectrum must be taken into account.

3.2. Main sources of FM-to-AM conversion

Dispersion is the primary cause of FM-to-AM conversion in fiber front-end systems, including GVD[8,22] and PMD[9,10]. This dispersion leads to phase-mismatch type modulation.
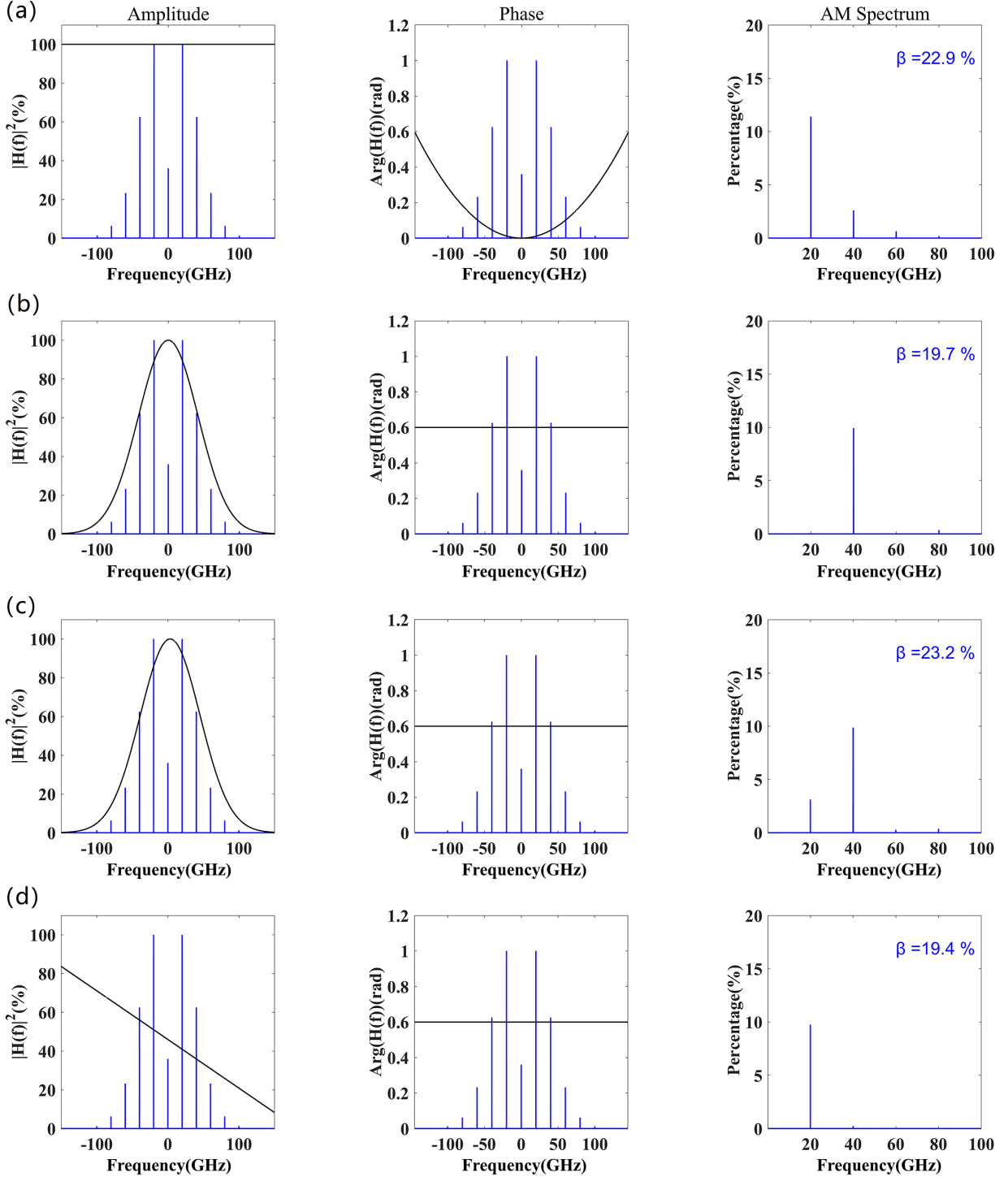
Figure 4. AM spectrum of several transfer functions: (a) pure phase transfer function; (b) symmetric exponential amplitude transfer function; (c) asymmetric exponential amplitude transfer function; (d) linear amplitude transfer function.

In addition, the front-end fiber amplifiers, neodymium glass regeneration and pre-amplifiers and main amplifiers generate amplitude-mismatch type modulation, resulting in gain narrowing effects[10,23]. The FM-to-AM conversion caused by nonuniform amplitude transmission can be compensated by using appropriate filters. Lyot filters based on birefringent crystals and polarization devices[24,25] can flatten the gain profile by polarization-dependent attenuation. In addition, the Fabry–Pérot (F-P) etalon effect, spatial filter and CPP spatial shaping may also cause certain FM-to-AM conversion. The analysis diagram of the factors influencing FM-to-AM conversion in the SG II-Up facility is shown in Figure 5.
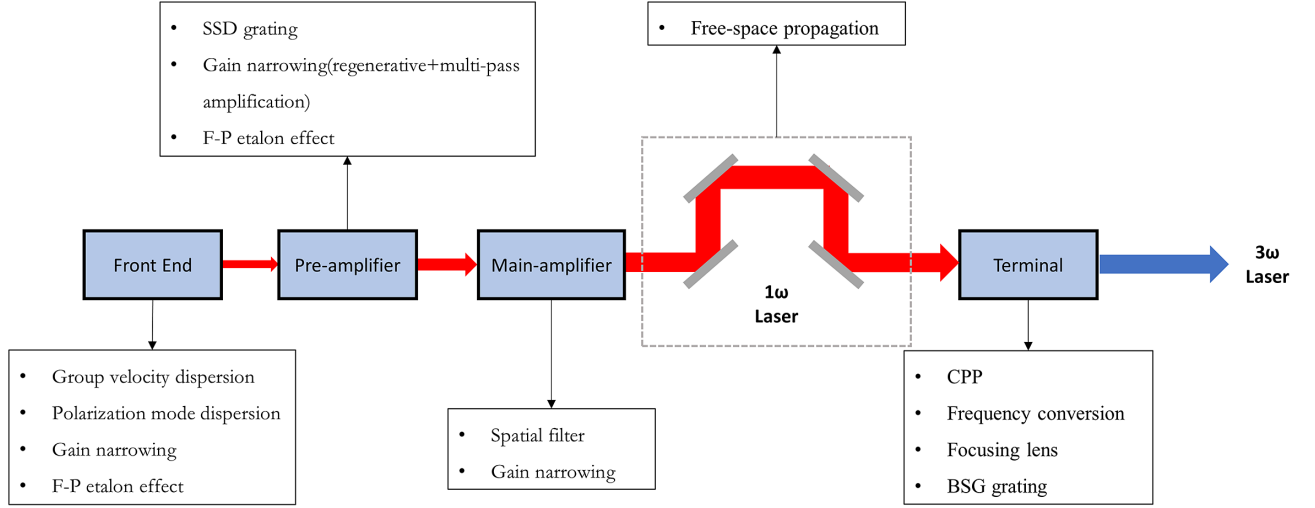
Figure 5. Analysis diagram of FM-to-AM influencing factors of the high-power laser facility.

3.2.1. Influencing factors of the phase transfer function

Polarization mode dispersion. Due to the birefringence effect of the PMF, laser pulses with two polarization components perpendicular to each other are transmitted in the fiber with a certain time delay, which is known as the differential group delay (DGD). The polarization extinction ratio (PER) of the currently used commercial PMF is as high as 40–50 dB, but due to the presence of fiber connectors, fusion joints, etc., at the end of the fiber, the extinction ratio may degrade to approximately 20 dB. If the connection between the PMFs cannot ensure the alignment of the fast and slow axes, some of the light will not transmit in the same polarization state as the incident light, resulting in depolarization. Using the Jones matrix method, the transfer function of the fiber connector and the PMF on the signal can be deduced:

$$H(f) = 1 + \frac{1}{P}\exp\left[-i(2\pi f \Delta\tau + \varphi)\right], \qquad (20)$$

where P is the PER of the input and output fiber connectors, $\Delta\tau$ is the DGD and φ is the phase difference between the fast and slow axes.

It has been shown that single-polarization fiber can effectively suppress PMD. In October 2016, the NIF reported they had successfully solved FM-to-AM conversion problem caused by PMD by using single-polarized transmission fiber and single-polarized gain fiber[14]. The front-end system of ninth beam of the SG II-Up facility has also utilized single-polarization transmission fiber to mitigate the PMD since 2021. With the exception of the ytterbium-doped fiber, all other fiber components are constructed using domestic single-polarization fiber (developed by the 46th Research Institute of the China Electronics Technology Group Corporation) and single-polarized fiber devices.
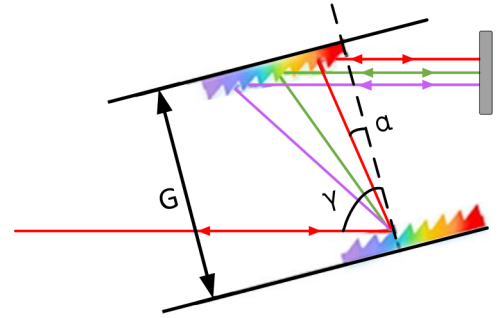

Figure 6. Schematic diagram of dispersion compensation for the parallel grating pair.

The length of ytterbium-doped fiber used in the single fiber amplifier is 2 m. According to the simulation analysis, when the input laser polarization is 20 dB, a temperature change of 10°C results in a 2.1% FM-to-AM conversion caused by PMD in the polarization-maintaining ytterbium-doped fiber[26].

Group velocity dispersion and compensation. The GVD is caused by the phase mismatch resulting from the inconsistent transmission velocities of different spectral components in the fiber. The relative transmission function can be expressed as follows[8]:

$$H(f) = \exp\left(-i\beta_2 L\omega^2\right), \qquad (21)$$

where β_2 is the effect of GVD. The intensity of the output pulse after GVD can be expressed as follows:

$$I_{\text{out}}(t) = 1 + 2\beta_2 L\left[m_1\omega_1^2\sin(\omega_1 t) + m_2\omega_2^2\sin(\omega_2 t)\right]. \quad (22)$$

For the compensation of GVD, a parallel grating pair is usually used[27] (as shown in Figure 6). The compensation principle is as follows: after the incident light is dispersed by the grating, the long-wavelength component takes more
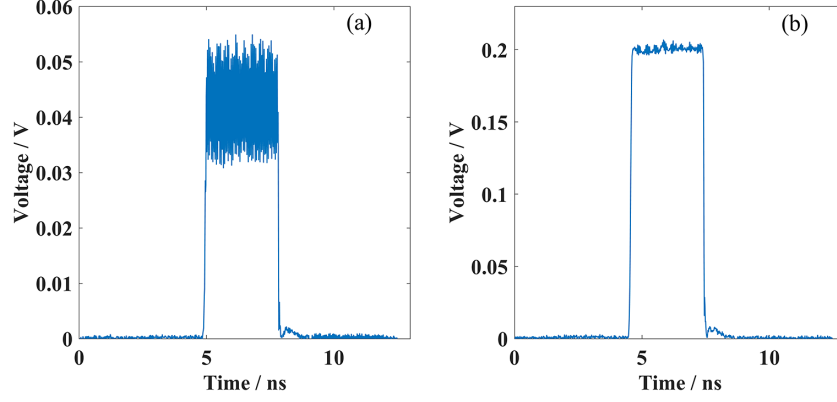
Figure 7. Temporal modulation (a) before and (b) after GVD compensation for 0.3 nm @ 3 GHz + 20 GHz phase modulation.

time to pass through the grating pair compared to the short-wavelength component. Appropriate selection of the angle of incidence and grating parameters can produce negative GVD.

The amount of dispersion introduced by the parallel grating pair is as follows:

$$D = \frac{G\lambda_0}{cd^2\cos^3\left[\alpha\left(\lambda_0\right)\right]}, \tag{23}$$

where d is the grating constant and G is the grating spacing. The incident angle γ and $\alpha\left(\omega\right)$ satisfy the grating equation $\sin\gamma + \sin\left[\alpha\left(\omega\right)\right] = \frac{2\pi c}{\omega d}$.

In the actual device, the various pulses generated by the arbitrary waveform generator (AWG) are selected using the time-division multiplexing (TDM) method, resulting in a specific time delay between each pulse. In order to achieve an equal optical path to the target, the length of the transmission fiber varies. The single-polarization transmission fiber used is from the 46th Research Institute of the China Electronics Technology Group Corporation, which has a dispersion coefficient of 37.2 ps^2/km. The length of the fiber ranges from 100 to 150 m. The introduced GVD is about 6.33–9.49 ps/nm, and the compensated GVD is 1.87–5.03 ps/nm. In order to ensure the consistency of the GVD compensation unit and compensate for the different GVD caused by different fiber lengths, the incidence angle adjustment range of the grating is designed to be 5°. Figure 7 shows the FM-to-AM conversion before and after the dispersion compensation. The addition of the dispersion compensation unit reduces the modulation degree from 28.1% to 2.4%. We currently consider that the main source of the remaining modulation degree is the PMD caused by the PMF in the fiber amplifier.

SSD grating. SSD gratings can be used to spatially separate different wavelengths by introducing spatial dispersion, which causes dephasing of the sidebands. As a result, the cumulative phase varies for each wavelength after the

grating, which causes the temporal AM. In the case of free-space propagation, the intensity at a plane a distance z from the grating is as follows[12]:

$$I\left(y,z,t\right) = \frac{I_0}{1 + \frac{m\varepsilon^2 z}{k_0}\sin\left[\omega_m t + \varepsilon y_0\left(y,z,t\right)\right]}. \tag{24}$$

The angular scatter is $\frac{\Delta\theta}{\Delta\lambda}$ and the spectral angular scatter is $\varepsilon = 2\pi\frac{\Delta\theta}{\Delta\lambda}\frac{\omega_m}{\omega_0}$. Therefore, the modulation degree is as follows:

$$\beta_{\mathrm{g}}(z) = \frac{m\varepsilon^2 z}{k_0}. \tag{25}$$

There exists a critical distance z_{r} at which the intensity tends to infinity, $z_{\mathrm{r}} = \frac{k_0}{m\varepsilon^2}$.

For a propagation distance z behind the plane grating in the case of the Littrow configuration at the angle θ_0, we have for the center frequency f_0, with a density of grooves N:

$$\left.\frac{\Delta\theta}{\Delta\lambda}\right|_{\theta=\theta_0} = \frac{N}{\cos\left(\theta_0\right)}. \tag{26}$$

Then

$$\beta_{\mathrm{g}}(z) = \frac{2\pi cN^2 z}{f_0^3\cos^2\left(\theta_0\right)}mf_m{}^2. \tag{27}$$

After the SSD grating, the modulation degree is proportional to the transmission distance.

3.2.2. Influencing factors of the amplitude transfer function

Gain narrowing. The amplifier, as the core component of the high-power solid-state laser driver, is the key factor in obtaining a high-quality beam. The amplification system mainly consists of rod amplifiers, disk amplifiers, spatial filters, isolators and multiple reflectors. However, intensity modulation is caused by the spectral selectivity resulting from the gain spectrum of the amplification medium. The pre-amplified laser beam passes through the transmission

spatial filter (TSF) twice and the cavity spatial filter (CSF) four times before entering the final optics and target field.

When an optical pulse is transmitted through a gain medium, the phenomenon that the laser bandwidth is reduced due to nonuniform amplification is called the gain narrowing effect. Therefore, the spectrum of the laser pulse after amplification can be expressed as follows[28]:

$$E_{\text{out}}(\omega) = E_{\text{in}}(\omega) G(\omega)^n, \qquad (28)$$

where $G(\omega) = e^{gl}$ represents the frequency gain, l represents the gain length of the medium, n represents the number of amplification range and g represents the gain coefficient. This equation is applicable to a working medium with a uniformly broadened Lorentzian line pattern:

$$g = g_0(\omega_0) \frac{1}{1 + \frac{4(\omega - \omega_0)^2}{\Delta\omega_{\text{H}}^2}}, \qquad (29)$$

where $g_0(\omega_0)$ is the small signal gain at the center frequency and $\Delta\omega_{\text{H}}$ is the gain bandwidth of the medium.

According to the simulation results, in the case of phase modulation with single frequency, the FM-to-AM conversion is primarily caused by an even multiple of f_m when there is a symmetric gain line centered around the carrier frequency. Conversely, it is caused by an odd multiple of f_m.

Spatial filter. A spatial filter is a technique used to improve the quality of the laser and is equivalent to a low-pass filter[3]. The spectrally dispersive beam is spatially dispersed by the grating in the x-direction, and the optical field can be expressed as follows:

$$E_x(x,t) = \exp\left[im\sin(2\pi f_m t) - i\left(\frac{\omega_t}{c}\right)x\sin\theta\right], \qquad (30)$$

where the instantaneous frequency $\omega_t = \omega_0 + 2\pi m f_m \cdot \cos(2\pi f_m t)$, $\theta = \frac{\Delta\theta}{\Delta\lambda}\frac{\lambda}{\omega_0}2\pi m f_m \cos(2\pi f_m t)$.

Since the spatial filter pinhole is located in the far field of the laser system, the distribution at the pinhole can be obtained through Fourier transform:

$$E(u,t) = T(x)\text{FFT}([E_x(x,t)]), \qquad (31)$$

$$T(x) = \begin{cases} 1, & x < \text{radius} \\ 0, & x > \text{radius} \end{cases}. \qquad (32)$$

The intensity can be calculated by integrating the following:

$$I(t) = \int |E(u,t)|^2 \, du. \qquad (33)$$

If the divergence angle θ_4 of the target surface is known, then $f_3\theta_4 = f_2\theta_2$, $f_1\theta_1 = f_2\theta_2$ and $\theta_1 = 98.28$ μrad, $\theta_2 = 11.73$ μrad, where $f_{i(i=1,2,3)}$ are the focal lengths of the lenses and $\theta_{i(i=1,2,3)}$ are the spreading distances between the edge frequency and fundamental frequency at the focal point of the lens (as shown in Figure 8). Therefore, the pinhole size

satisfies $2r_1/f_1 \geq 2\theta_1$, $2r_2/f_2 \geq 2\theta_2$, $r_1 = r_2 \geq 263.96$ μm[13], where r_1, r_2 represent the radius of the pinhole. For TSF-1, the beam aperture is 310 mm, the TSF-L1 focal length is 22.5 m and the diffraction limit is $\text{DL}_1 = 2\lambda_0 f_1/D_1 = 152.9$ μm. The pinhole size is chosen to be $30\text{DL}_1 = 4.59$ mm, so that the FM-to-AM conversion caused by the spatial filter is about 0.093%. Similarly, the modulation degree caused by the second spatial filter through the TSF is 0.043%.

The two focal lengths of the CSF lenses are 11,883 and 11,177 mm, respectively, in the SG II-Up facility. The beam apertures for each pass of the laser are 310 and 290 mm. The aperture size of the CSF is 60 times the diffraction limit. The FM-to-AM conversion introduced during the four passes through CSF-L1 and CSF-L2 is shown in Table 1.

CPP spatial shaping. The CPP is a phase-dependent element designed to address the phase-recovery problem. The Fourier transform and inversion can be used to reconstruct the phase distribution of the object field and obtain the desired output field. This technique allows for shaping the far-field focal spot while still meeting the constraints of the image field. The SSD beam can produce $N = 2m + 1$ mutually independent far-field Airy spots, and the distance between adjacent Airy spots is $N_c D_{\text{lim}}$. SSD combined with the CPP will alter the position of the local speckle, which only affects the distribution of the speckles and does not impact their size. Assuming that the intensity inhomogeneity of a single speckle is δ_{rms0}, the superposition of N speckles with the same intensity, independent of each other, will enhance the uniformity of $\delta_{\text{rms}} = \delta_{\text{rms0}}/\sqrt{N}$ (where δ_{rms} is defined mathematically in Equation (34)). However, in this paper, the impact of CPP spatial shaping on time-domain modulation will be analyzed:

$$\delta_{\text{rms}} = \left\{ \frac{\iint_A \left[I(x,y) - I_{\text{obj}}(x,y)\right]^2 dx dy}{\iint_A \left[I_{\text{obj}}(x,y)\right]^2 dx dy} \right\}^{1/2}, \qquad (34)$$

where A is the statistical region, $I(x,y)$ is the intensity and $I_{\text{obj}}(x,y)$ is the average intensity in the statistical region.

In the absence of the CPP, the far-field distribution on the focal plane can be expressed as follows:

$$\sum_{n=-m}^{m} \exp(-i2\pi n f_m t) \left[J_n(m) E_{\text{airy}}(x_{\text{FF}}, y_{\text{FF}} - n N_c D_{\text{lim}})\right]. \qquad (35)$$

The far-field distribution after CPP shaping can be expressed as follows:

$$\sum_{n=-m}^{m} \exp(-i2\pi n f_m t) \left[J_n(m) E_{\text{cpp}}(x_{\text{FF}}, y_{\text{FF}} - n N_c D_{\text{lim}})\right]. \qquad (36)$$
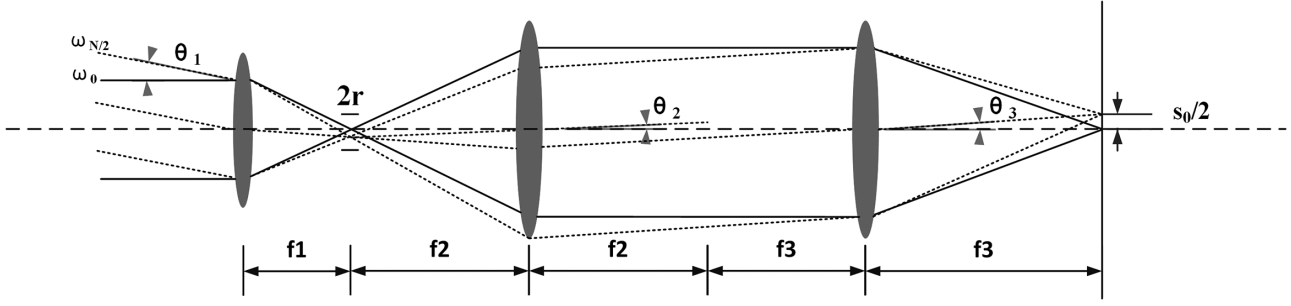
Figure 8. Principle of pinhole aperture selection.

Table 1. Spatial filters parameters and FM-to-AM caused by the pinhole.

Spatial filter[a]	Input lens focal length (mm)	Incident beam aperture (mm)	Pinhole aperture (μrad)	FM-to-AM modulation
TSF-1	22,500	310	±101.9	0.093%
TSF-2	22,500	310	±203.8	0.043%
CSF-1	11,883	310	±203.8	0.087%
CSF-2	11,117	290	±217.9	0.080%
CSF-3	11,883	310	±203.8	0.087%
CSF-4	11,117	290	±217.9	0.080%
Total	——	——	——	0.2%

[a]The first column represents the hole number of the spatial filter.

Equations (35) and (36) show that, regardless of the presence of the CPP, each frequency component of the far-field distribution corresponds to a relative amplitude $J_n(m)$. The CPP only affects the results of spatial shaping and does not affect the sideband dephasing of the SSD beam, so it does not introduce additional FM-to-AM conversion. It can be seen from the simulation that the FM-to-AM conversion from CPP spatial shaping is $10^{-13}\%$ and does not affect the time-domain modulation.

Frequency conversion. The FM-to-AM comes from two aspects during frequency conversion. Firstly, the frequency conversion process is related to the incident intensity, and the AM depth of 1053 nm will be amplified. Secondly, the filtering effect of the transfer function is affected by the phase mismatch in the nonlinear crystal. In the case of perfect spectral phase matching, the generation of low-intensity third harmonics is satisfied[5,29]:

$$\beta_{3\omega} = 3\beta_{1\omega}. \tag{37}$$

The time-domain relationship of the third harmonic generation (THG) after frequency conversion is as follows:

$$I_{3\omega}(t) = 1 + 2\beta_2 L\left[3m_1\omega_1^2\sin(\omega_1 T) + 3m_2\omega_2^2\sin(\omega_2 T)\right]. \tag{38}$$

The phase mismatch causes spectral distortion, assuming there is no plane grating for SSD and considering the classical equation for the frequency conversion of the THG in the low-intensity case[5]:

$$A_3(\Delta k) = A_{3\text{max}} e^{\frac{i\Delta kL}{2}} \text{sinc}\left(\frac{\Delta kL}{2}\right). \tag{39}$$

Assuming that the phase mismatch is proportional to the frequency, the frequency conversion of the phase mismatch can be interpreted as a linear filter of A_3. Under the same assumptions, the complex exponent in the above equation represents a time delay that does not produce AM. Therefore, the AM resulting from phase mismatching is only due to the second part. We can express the effective transfer function for the FM-to-AM conversion as follows:

$$H_{\text{fc}}(f) = 1 - \frac{\gamma^2}{6}(f - f_{\text{c}})^2. \tag{40}$$

Its modulation degree is as follows:

$$\beta_{\text{fc}} = \frac{\frac{\gamma^2}{6}(f_{\text{c}} + 3m_1 f_{m1} + 3m_2 f_{m2})^2}{1 - \frac{\gamma^2}{6}(f_{\text{c}} + 3m_1 f_{m1} + 3m_2 f_{m2})^2}. \tag{41}$$

Taking the phase mismatch into account, it is known that the spectral distortion caused by frequency conversion in the THG can be expressed as follows:

$$I_{\text{fc}}(t) = I_{3\omega}(t)\left\{1 - \frac{\gamma^2}{6}\left[3m_1 f_{m1}\cos(2\pi f_{m1}t) + 3m_2 f_{m2}\cos(2\pi f_{m2}t)\right]^2\right\}. \tag{42}$$
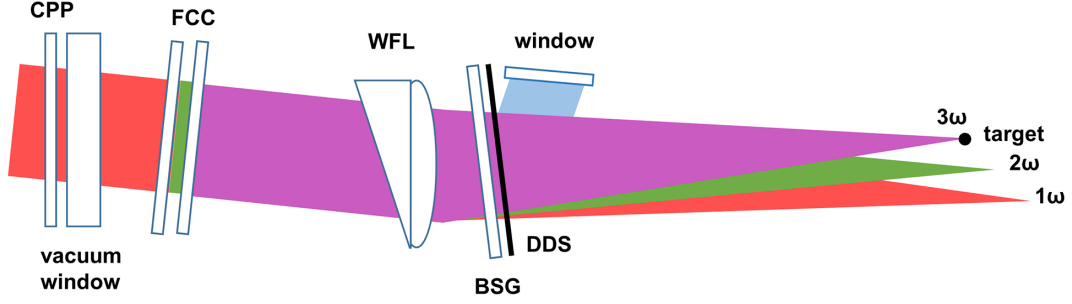
Figure 9. Configuration of the final optics components of the SG II-Up facility.

3.3. The focusing lens causes a reduction in the modulation degree

During the transmission of the beam through the reflection system to the WFL, the long-wave component arrives before the short-wave component due to the different propagation speeds of the broad spectrum, resulting in a time delay: $t_{\text{reflect}} = \frac{\Delta n \cdot L_{\text{total}}}{c} = \frac{\Delta n}{\Delta \lambda} \Delta \lambda \frac{L_{\text{total}}}{c} = 0.526$ ps, where $\Delta \lambda = 0.1$ nm @ 351 nm.

In order to separate the unconverted 1ω and 2ω light, a WFL is adopted in the SG II-Up facility (Figure 9). The spectrum broadened beam will diverge when passing through the wedge-shaped plate. According to Sellmeier's formula, the refractive index of the quartz material varies with wavelength as follows:

$$n^2 = A + \frac{B}{\lambda^2 - C} - D\lambda^2, \qquad (43)$$

where the *ABCD* numbers of the quartz material are $A = 2.35685106367076$, $B = 0.0107275417314043$, $C = 0.00983583625003204$ and $D = 0.0114164989926211$. After passing through a wedge-shaped plate of length l, the time delay is $t_{\text{d}} = \frac{l\Delta n}{c}$:

$$\frac{\Delta n}{\Delta \lambda} = \frac{1}{2n} \left[\frac{-2B\lambda}{(\lambda^2 - C)^2} - 2D\lambda \right]. \qquad (44)$$

Therefore, $t_{\text{d}} = \frac{l\Delta\lambda}{c} \frac{\Delta n}{\Delta\lambda} = 4.96 \times 10^{-3}$ ps, which is very small compared to the time delay of 81.2 ps generated by the SSD grating and has minimal impact on temporal AM.

For a spatially flat-top beam passing through a grating, the far-field intensity can be related to the near-field intensity by the following expression[5]:

$$I_{\text{ff}}(t) = \iint I_{\text{fc}} \left[t - \delta t(x, y) \right] \mathrm{d}x\mathrm{d}y. \qquad (45)$$

After being focused by a WFL, the lens acts as an integrator in the focal plane. The grating generates a time delay proportional to the spatial position. Due to the time delay, the far-field intensity is temporally averaged. If there is a

modulated waveform due to FM-to-AM conversion, the AM will be reduced as a result of temporal integration.

4. Simulation of frequency modulation-to-amplitude modulation conversion of the SG II-Up facility

4.1. AM spectrum with 3 GHz phase modulation

Considering only 3 GHz modulation with a bandwidth of 0.15 nm and modulation levels of 2% or 5% after the main amplifier, the FM-to-AM conversion is shown in Figure 10. Figures 10(a)–10(d) represent the FM-to-AM conversion on the surface of the last transmission mirror, the incident surface of the WFL, the surface of the BSG and the target, respectively. It can be observed that the spectrum of the 3 GHz phase modulation after tripling is primarily composed of the fundamental-frequency component at 3 GHz, followed by the second harmonic component at 6 GHz if FM-to-AM is well controlled in the front end, pre-amplification and main amplification. The analysis in Section 4.2 demonstrates that the combined effect of the dispersive grating and the focusing system is equivalent to a band-pass filter with an 8 GHz 3 dB bandwidth. In addition, the decrease in modulation degree is contingent upon the amplitude spectrum modulation, which is influenced by the phase modulation frequency and amplitude or phase changes of the spectrum. For phase modulation only at 3 GHz, even after frequency conversion, the AM spectrum remains below the low-pass cutoff frequency of the filter. Therefore, the phase-modulated beam with 3 GHz does not cause a significant decrease in the modulation degree after passing through the WFL. The modulation degree of the phase-modulated laser at 3 GHz freely transmitted to each transmission mirror and the incident surface of the final optics is shown in Table 2.

At present, the FM-to-AM conversion after the main amplifier of the SG II-Up facility is 3.5% and 5% without and with the SSD (~0.3 nm @ 3 GHz + 20 GHz) grating[18], respectively. The transmission of the target laser mainly consists of 16 nanosecond laser pulses. By utilizing eight beam splitter elements, the eight beams of the fundamental-frequency laser output from the main amplifier system are divided into 16 beams. Each beam is then transmitted to the
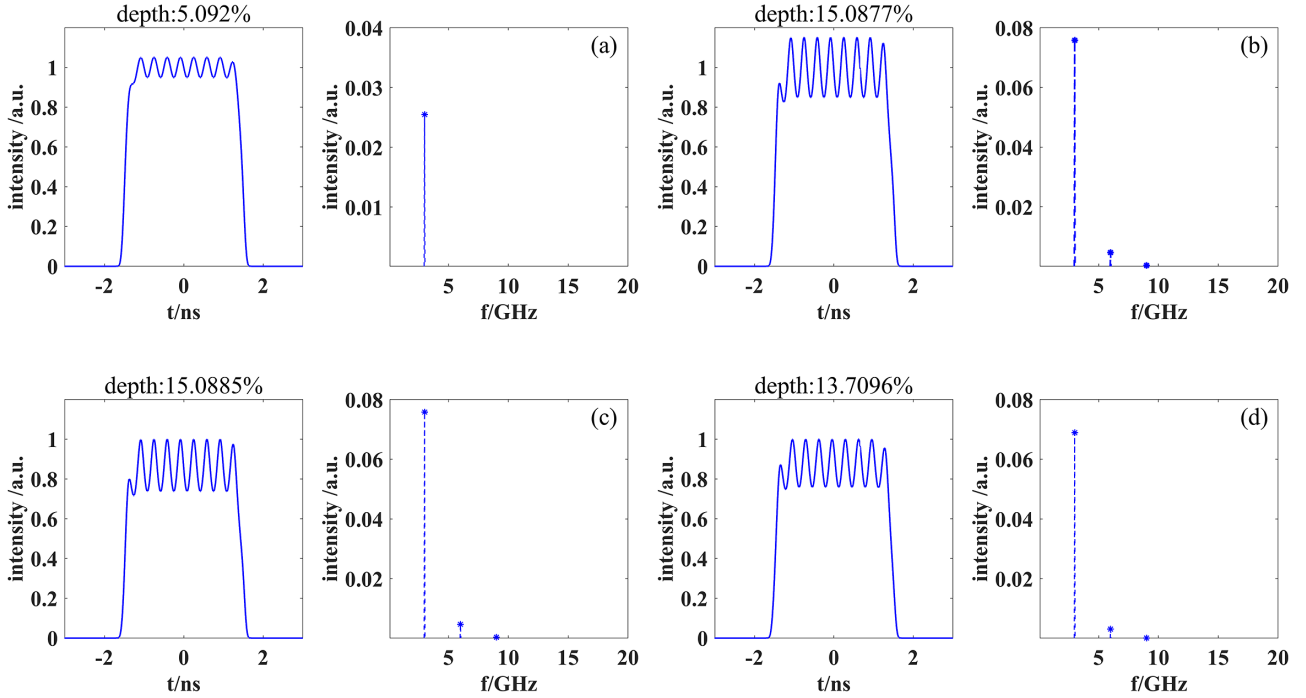
Figure 10. When the FM-to-AM is 5% @ 3 GHz, 0.15 nm after the main amplifier, the FM-to-AM on the subsequent optical components and the target surface: (a) last transmission reflector surface; (b) incident surface of the WFL; (c) BSG; (d) target.

Table 2. FM-to-AM conversion of laser free transmission to the surface of each transmission mirror and the incident surface of the final optics.

	Spacing (mm)	Modulation
After main amplifier		5%
WP[a]	500	4.996%
TM1	8970.1	5.020%
TM2	2683.8	5.028%
TM3	10,216.3	5.056%
TM4	5103.4	5.070%
TM5	6450.2	5.088%
TM6	1608	5.092%
CPP	2783.5	5.100%
Vacuum window	10	5.100%
FCC	60	5.100%
WFL	612.5	15.088%
BSG	306.9	15.089%
Target	2005.6	13.710%

[a]WP represents the wedge plate.

FOA by using either five (for the beam splitter reflection beam) or six (for the beam splitter transmission beam) large-aperture 1ω reflectors. Consider the transmission in the reflection part and choose one of the beams. The optical path between each reflector is shown in Table 2. Firstly, consider the 3 GHz phase modulation. Eliminating the 50 μm modulation of the target surface requires the grating role dispersion $\frac{\Delta\theta}{\Delta\lambda} = 770.91$ μrad/nm. After amplification of the grating, the role dispersion becomes 74.605 μrad/nm, with an amplification of 8.38. Based on the two modulation degrees of 2% and 5%, Table 2 shows the FM-to-AM

conversion of the laser on each transmission reflector and the incident surface of the final optics.

As can be seen in Table 2, at present, with better control of the front end, pre-amplification and main amplification, the FM-to-AM conversion can be well controlled near 2% @ 3 GHz. However, it can sometimes be worsened to 5% @ 3 GHz due to various incidental reasons in the system.

4.2. AM spectrum with 3 GHz + 20 GHz phase modulation

For the SG II-Up facility, if the phase modulation is 3 GHz + 20 GHz, most of the AM will be generated by 20 GHz. The modulation degree, including compensation for GVD and gain narrowing, can be controlled to approximately 5% from the front end to the main amplifier. Figure 11 shows the verification on the High Energy Integrated Laser Beam of the SG II-Up facility. It can be seen that the FM-to-AM conversion after the main amplifier is about 5%. Figure 12(a) shows the temporal waveform and intensity spectrum of 1ω. The main spectral components that affect the modulation degree are 3 and 20 GHz, with the proportion of each spectral component being 6.98% for 3 GHz and 93.02% for 20 GHz. It can be observed that the main source of AM is the modulation frequency of 20 GHz. However, this will be partially filtered out by the focusing system. Figure 12(b) displays the temporal waveform and intensity spectrum on the incident surface of the WFL. It is evident that after frequency conversion, the impact of modulated frequency components of the sum frequency, difference frequency and
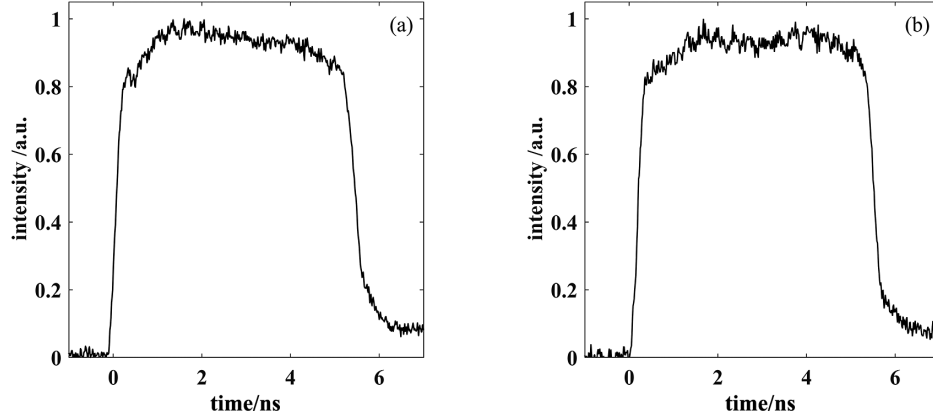
Figure 11. Time-domain modulation (measured by an Agilent DSO93004L with 30 GHz and an EOT ET-3600 with 22 GHz) at different wavelengths for the High Energy Integrated Laser Beam of the SG II-Up facility: (a) wavelength at 1052.5 nm (4.3%); (b) wavelength at 1053 nm (4.9%).
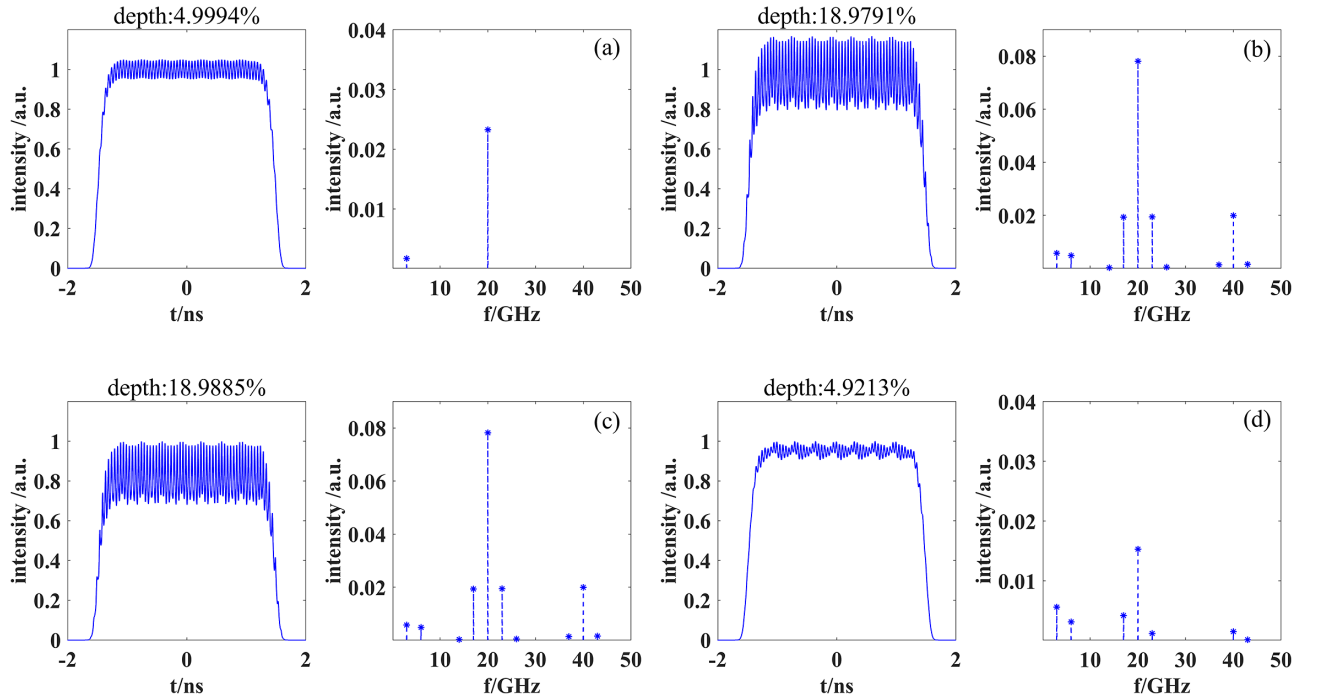

Figure 12. Phase modulation with 3 GHz + 20 GHz: (a) after the main amplifier (1ω); (b) incident surface of the WFL; (c) BSG; (d) target.

multiple-frequency of 20 GHz on the FM-to-AM conversion increases, surpassing even the 3 GHz FM-to-AM modulated frequency.

Figure 12(c) shows the temporal modulation caused by FM-to-AM conversion on the surface of the BSG. In ICF, to meet the high energy requirements of the target and to mitigate any instability that may occur during the compression of the target sphere, it is necessary to utilize beam sampling elements. These elements are used to sample the triplet frequency laser, allowing for the diagnosis of the energy, spatial distribution and temporal waveform. The commonly used sampling element is the BSG. The modulation due to grating dispersion needs to be taken into account. The BSG used in the SG II-Up facility is 2000 lines/mm, while

the Littrow angle is 10°. The distance from the grating to the target surface is 2.0056 m and the modulation at the target is 4.59%. The plane grating produces a frequency transfer function as a result of dispersion. Its AM spectrum has the highest percentage of first harmonic. Therefore, when comparing Figure 12(c) to Figure 12(b), the main difference is an increase in the percentage of the spectral component at 20 GHz, which causes a rise in the modulation degree. Figure 12(d) shows the time waveform and intensity spectrum of the FM-to-AM conversion at the target.

In the SG II-Up facility, the total time delay comes from the SSD grating, the WFL and the color separation. The final temporal modulation on the target is approximately 3.6%. The main frequency components that affect the modulation

Table 3. Proportion of each frequency modulation component before and after focusing.

Spectral component	3 GHz	6 GHz	17 GHz	20 GHz	23 GHz	40 GHz
Before focusing	0.68%	0.78%	3.09%	9.14%	3.11%	3.17%
After focusing	0.64%	0.60%	0.80%	1.70%	0.23%	0.27%
Transmission rate	0.97	0.65	0.22	0.20	0.06	0.075
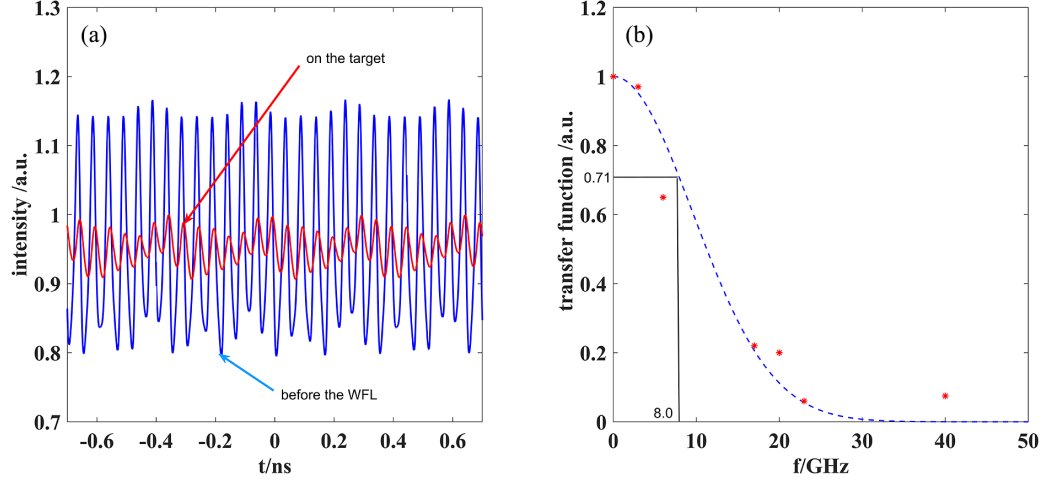
Figure 13. (a) Temporal modulation before (blue) and after (red) the WFL; (b) AM spectral transfer function.

degree and their proportion are shown in Table 3. When comparing the frequency components before and after focusing, it is evident that, apart from the fundamental frequency and multiple frequency at 3 GHz, the other spectral components exhibit a significant decrease. The decreasing trend follows a Gaussian form (Figure 13). Therefore, the transfer function is fitted with a Gaussian function $H_t = \exp\left(-\frac{x^2}{2D_0^2}\right)$, where $D_0 = 9.56$ GHz (standard deviation). This AM filter reduces the intensity modulation of the target and is equivalent to a Gaussian low-pass filter with 8 GHz (–3 dB bandwidth). The attenuation of the AM spectrum depends on the number of color cycles N_c, $N_c = f_m t_d$. That is, the transmittance of the frequency component below 8 GHz is higher than 70%, while the transmittance above 20 GHz is lower than 10%. As a result of this filtering, the AM spectrum of the phase modulation at 20 GHz, which helps to smooth the beam, is significantly reduced after passing through the WFL. Table 4 records the FM-to-AM conversion of the laser free transmission to each transmission reflector and the incident surface of the final optics under phase modulation with 3 GHz + 20 GHz.

5. Conclusion

In high-power laser drivers, near-field modulation and far-field smoothness are two key factors to consider. The former affects the damage of the final optics, while the latter directly affects the interaction between the laser and the target. In fact, we also need to pay attention to time-domain modulation, which is the smoothness of the time–power

Table 4. FM-to-AM conversion of laser free transmission to the surface of each transmission mirror and the incident surface of the final optics.

	Spacing (mm)	Modulation
After main amplifier		~5%
WP[a]	500	5.000%
TM1	8970.1	5.353%
TM2	2683.8	5.459%
TM3	10,216.3	5.862%
TM4	5103.4	6.063%
TM5	6450.2	6.317%
TM6	1608	6.381%
CPP	2783.5	6.490%
Vacuum window	10	6.491%
FCC	60	6.493%
WFL	612.5	18.979%
BSG	306.9	18.989%
Target	2005.6	4.921%

[a]WP represents the wedge plate.

curve. In addition, FM-to-AM conversion is the key factor affecting the smoothness of the time–power curve and it will increase the risk of damage to final optics components and affects the interaction between the laser and target. However, the modulation degree is not sufficient to quantify the effect of FM-to-AM conversion, and the intensity spectrum needs to be analyzed. In this paper, we analyze the FM-to-AM conversion generated by the full chain of the SG II-Up facility and explore the main spectral component that affects the modulation degree on the final optics and the target. The results indicate the following.

(1) When using only 3 GHz phase modulation, the FM-to-AM conversion can be controlled within 2.5% from the

front end to the main amplifier. In addition, the maximum modulation is on the WFL, which is approximately 5.8%. The temporal modulation is approximately 5.3% on the target. Specifically, the modulation degree caused by 3 GHz is 4.77%, which accounts for 90% of the total modulation.

(2) Under the phase modulation of 3 GHz + 20 GHz, the FM-to-AM conversion can be controlled to within 5% from the front end to the main amplifier. In this case, the modulation degree on the incident surface of the WFL is 19%, while on the target surface it is 4.9% due to the combination of the dispersive grating and the focusing system. It is worth noting that 50% of the modulation degree is attributed to 20 GHz.

(3) Most of the AM is generated by the modulation of a high frequency of 20 GHz, which can be controlled to be approximately 5% from the front end to the main amplifier. Other sum, differential and multiple frequency components are generated by frequency conversion in front of the WFL, which will greatly affect the AM. However, the combination of the dispersive grating and the focusing system is equivalent to a Gaussian low-pass filter with an 8 GHz 3 dB bandwidth. The transmittance of the spectral component at 20 GHz is less than 15%, and the high-frequency component is greatly filtered out.

The above results provide a key basis for monitoring FM-to-AM conversion, evaluating the load of terminal optical components and evaluating the effect of interaction between the laser and target during the operation of high-power laser facilities for ICF.

Acknowledgement

References

1. P. Perez-Martin, I. Prencipe, M. Sobiella, F. Donat, N. Kang, Z. He, H. Liu, L. Ren, Z. Xie, J. Xiong, Y. Zhang, F.-E. Black, M. Cervenák, P. Gajdoš, L. Hronová, K. Kaniz, M. Kozlová, F. Kroll, X. Pan, G. Schaumann, S. Singh, M. Šmíd, F. Suzuki-Vidal, P. Zhang, J. Sun, J. Zhu, M. Krus, and K. Falk, High Power Laser Sci. Eng. **11**, e17 (2023).
2. R. Betti and O. A. Hurricane, Nat. Phys. **12**, 435 (2016).
3. H. Zhang, S. Zhou, Y. Jiang, J. Li, W. Feng, and Z. Lin, Chin. Opt. Lett. **10**, 060501 (2012).
4. S. Hocquet, E. Bordenave, J. P. Goossens, C. Gouedard, L. Videau, and D. Penninckx, J. Phys. Conf. Ser. **112**, 032016 (2007).
5. S. Hocquet, D. Penninckx, E. Bordenave, C. Gouedard, and Y. Jaouen, Appl. Opt. **47**, 3338 (2008).
6. D. S. Montgomery, Phys. Plasmas **23**, 055601 (2016).
7. J. Huang, W. Fan, Z. Shi, X. Pan, R. Li, X. Lu, X. Wang, and S. Zhang, Acta Photon. Sin. **47**, 0914006 (2018).
8. R. Li, W. Fan, Y. Jiang, Z. Qiao, P. Zhang, and Z. Lin, Appl. Opt. **56**, 993 (2017).
9. Z. Qiao, X. Wang, W. Fan, X. Li, Y. Jiang, R. Li, C. Huang, and Z. Lin, Appl. Opt. **55**, 8352 (2016).
10. B. Liao, "Theoreetical study of FM-AM issue on ICF facility," Master Thesis (University of Chinese Academy of Sciences, 2000).
11. P. Li, W. Wang, J. Su, and X. Wei, High Power Laser Sci. Eng. **7**, e21 (2019).
12. J. H. Kelly, A. Shvydky, J. A. Marozas, M. J. Guardalben, B. E. Kruschwitz, L. J. Waxer, C. Dorrer, E. Hill, A. V. Okishev, and J. M. Di Nicola, Proc. SPIE **8602**, 86020D (2013).
13. J. Li, H. Zhang, S. Zhou, W. Feng, J. Zhu, and Z. Lin, Acta Opt. Sin. **30**, 827 (2010).
14. https://lasers.llnl.gov/news/science-technology/2016/october.
15. M. L. Spaeth, K. R. Manes, D. H. Kalantar, P. E. Miller, J. E. Heebner, E. S. Bliss, D. R. Speck, T. G. Parham, P. K. Whitman, P. J. Wegner, P. A. Baisden, J. A. Menapace, M. W. Bowers, S. J. Cohen, T. I. Suratwala, J. M. Di Nicola, M. A. Newton, J. J. Adams, J. B. Trenholme, R. G. Finucane, R. E. Bonanno, D. C. Rardin, P. A. Arnold, S. N. Dixit, G. V. Erbert, A. C. Erlandson, J. E. Fair, E. Feigenbaum, W. H. Gourdin, R. A. Hawley, J. Honig, R. K. House, K. S. Jancaitis, K. N. LaFortune, D. W. Larson, B. J. Le Galloudec, J. D. Lindl, B. J. MacGowan, C. D. Marshall, K. P. McCandless, R. W. McCracken, R. C. Montesanti, E. I. Moses, M. C. Nostrand, J. A. Pryatel, V. S. Roberts, S. B. Rodriguez, A. W. Rowe, R. A. Sacks, J. T. Salmon, M. J. Shaw, S. Sommer, C. J. Stolz, G. L. Tietbohl, C. C. Widmayer, and R. Zacharias, Fusion Sci. Technol. **69**, 25 (2016).
16. D. Penninckx, N. Beck, J.-F. Gleyze, and L. Videau, J. Light-wave Technol. **24**, 4197 (2006).
17. D. Penninckx and N. Beck, Appl. Opt. **44**, 7773 (2005).
18. J. Guo, J. Wang, X. Pan, X. Lu, G. Xia, X. Wang, S. Zhang, W. Fan, and X. Li, Appl. Opt. **58**, 1261 (2019).
19. J. Chou, G. C. Valley, V. J. Hernandez, C. V. Bennett, L. Pelz, J. Heebner, J. M. Di Nicola, M. Rever, and M. Bowers, Proc. SPIE **8985**, 898511 (2014).
20. C. Huang, "Remote measurements and screening of FM-AM on high power laser," Master Thesis (University of Chinese Academy of Sciences, 2017).
21. M. Hohenberger, A. Shvydky, J. A. Marozas, G. Fiksel, M. J. Bonino, D. Canning, T. J. B. Collins, C. Dorrer, T. J. Kessler, B. E. Kruschwitz, P. W. McKenty, D. D. Meyerhofer, S. P. Regan, T. C. Sangster, and J. D. Zuegel, Phys. Plasmas **23**, 092702 (2016).
22. M. Sun, J. Kang, X. Liang, H. Zhu, Q. Yang, Q. Gao, A. Guo, P. Zhu, P. Zhang, L. Li, L. Qiu, Z. Lu, S. Wang, X. Tu, X. Xie, and J. Zhu, High Power Laser Sci. Eng. **11**, e2 (2023).
23. Y. Zobus, C. Brabetz, J. Hornung, J. B. Ohland, D. Reemts, J. Zou, M. Loeser, D. Albach, U. Schramm, and V. Bagnoud, High Power Laser Sci. Eng. **11**, e48 (2023).
24. K. Özgören and F. Ö. Ilday, Opt. Lett. **35**, 1296 (2010).
25. M. Fan, X. Tian, D. Zhou, J. Wei, H. Xia, H. Lv, H. Zhao, D. Xu, and W. Zheng, Photonic Sens. **11**, 325 (2021).
26. X. Qian, X. Wang, X. Lu, T. Zhang, and W. Fan, Appl. Sci. **12**, 884 (2022).
27. R. Ii, W. Fan, and Y. Jiang, "A fast-tunable dispersion compensation device based on parallel grating pairs," CN106329305A (January 11, 2017).
28. S. Zhao, Y. Wang, G. Chen, X. Wang, and X. Hou, Acta Photon. Sin. **26**, 197 (1997).
29. Y. Chen, L. Qian, H. Zhu, and D. Fan, Chin. Phys. Lett. **28**, 044209 (2011).